Biosensors and Bioelectronics 212 (2022) 114428

Contents lists available at ScienceDirect

Biosensors and Bioelectronics

journal homepage: www.elsevier.com/locate/bios

Enhanced chemiluminescence imaging sensor for ultrasensitive detection of nucleic acids based on HCR-CRISPR/Cas12a

Xinxin Ke [a], Yangjing Ou [b], Yu Lin [b], Tao Hu [a,*]

[a] The Children's Hospital, Zhejiang University School of Medicine, National Clinical Research Center for Child Health, Hangzhou, 310052, China
[b] International Peace Maternity & Child Health Hospital, Shanghai Municipal Key Clinical Specialty, Institute of Embryo-Fetal Original Adult Disease, School of Medicine, Shanghai Jiao Tong University, Shanghai, 200030, China

ARTICLE INFO

Keywords:
Chemiluminescence
CRISPR/Cas12a
Visual imaging
Hybridization chain reaction
Nucleic acids detection

ABSTRACT

CRISPR/Cas systems have ignited increasing attention in accurate and sensitive nucleic acids detection. In this work, we proposed the first CRISPR/Cas12a-based chemiluminescence enhancement biosensor by employing HCR amplifying strategy (CLE-CRISPR) for nucleic acids detection, which shows the advantages of high sensitivity and specificity, low-cost, visual imaging by comparison to reported biosensors. Upon the DNA target recognition, the activated CRISPR/Cas12a enabled randomly cutting initiator DNA (intDNA) into vast short products, which could not trigger the toehold-mediated DNA-strand displacement reaction (TSDR) with MB@crDNA. Thereby, the terminus of crDNA induced the hybridization chain reaction (HCR) with the coexistence of two hairpins (H1 and H2), forming a long double-stranded DNA framework. The attached streptavidin-AP yielded a conspicuous CL signal or visual imaging directly related to the DNA target concentration. The proposed CLE-CRISPR platform exhibited excellent sensitivity, with a relatively low detection limit at 3 pM for synthetic DNA target and single copy detection for plasmid by combining recombinase polymerase amplification (RPA) kit. We further validated the practical application of this platform using HPV clinical samples, achieving superior sensitivity and specificity of 88.89% and 100%, respectively. We believe that this work not only extends the application scope of CRISPR/Cas12a, but also devotes a new approach for clinical diagnosis.

1. Introduction

The current advent of clustered regularly interspaced short palindromic repeats (CRISPR)-Cas system has drawn mounting interests as it is considered a novel diagnostic tool due to its tunable nuclease activities (Dronina et al., 2021a; Feng et al., 2021; Horvath and Barrangou, 2010; Urdea et al., 2006; Yang et al. 2019, 2020b). Among the diverse CRISPR-Cas family, CRISPR-Cas12a is an endonuclease guided by a single CRISPR RNA (crRNA) and endows trans-cleavage ability on single-stranded DNA (ssDNA) upon recognizing a complementary double-stranded DNA (dsDNA) via a T-rich protospacer adjacent motif (PAM)-dependent manner or a complementary ssDNA activator in a PAM-independent manner (Ackerman et al., 2020; Chen et al., 2018; Gootenberg et al., 2017; Harrington et al., 2018; Pickar-Oliver and Gersbach, 2019; Ramachandran and Santiago, 2021; Teng et al., 2019). This feature makes CRISPR/Cas12a system a promising molecular diagnostic tool through converting targeted nucleic acids information into detectable signals. The initial application of CRISPR/Cas12a utilized a fluorophore quencher (FQ)-labeled ssDNA (ssDNA-FQ) as a signal interpretation (Chen et al., 2018; Li et al., 2019; Nouri et al., 2021). Once a specific target is recognized, the activated Cas12a randomly digested nonspecific ssDNA-FQ, unleashing a fluorescent signal which can be measured by virtue of fluoroanalyzer. Although optical transduction methods based on CRISPR/Cas12a show great potential for high sensitivity, single-base specificity, and point-of-care compatibility (Smith et al., 2020), further improvement is still necessary for broader readout types, higher sensitive means, and more practical applications.

On this matter, a variety of CRISPR/Cas12a-based biosensors have been constructed in terms of signal molecules tagged ssDNA or advanced analytical instruments, including colorimetry, electrochemistry (EL), electrochemiluminescence (ECL) (Dai et al., 2019; Ge et al., 2021; Hu et al., 2020; Jiang et al., 2021; Liu et al., 2022; Mukama et al., 2020; Wang et al., 2021; Yin et al., 2021; Zhang et al. 2021, 2022). Although EL and ECL methods exhibit high sensitivity and specificity, they are subjected to some defects, such as expensive electrode material and

* Corresponding author.
E-mail address: hutaozd@zju.edu.cn (T. Hu).

https://doi.org/10.1016/j.bios.2022.114428
Received 13 April 2022; Received in revised form 19 May 2022; Accepted 24 May 2022
Available online 27 May 2022

intricated pretreatment process, which are limited to convenient and cost-effective detection. It is simple and convenient for colorimetric means, while the sensitivity needs to be considered thoroughly. Accordingly, there is an urgent need to extend the CRISPR/Cas12a system toward the field of other biosensors.

Chemiluminescence (CL) has attracted overwhelming attention owing to its superior properties such as high sensitivity, simple instrumentation, rapid response, and CL imaging (Yahyai and Lawati 2021; Xu et al., 2019; Yang et al., 2020a). As is known to all, the CL signal of antibody coupled with HRP and AP catalytic systems have been applied to commercialized diagnosis tools (Kricka, 2003; Speletas et al., 2020). In addition, the CL biosensors of DNA labeled with native enzymes or mimic enzymes have also been developed for nucleic acids and small molecular detection, as well as bioimaging aspects (Hatakeyama et al., 2009; Mei et al., 2020). Recently, Mei et al., (2020) developed a CL platform for the detection of miRNA-21 using a probe DNA modified PtCuCo-TAs catalyzer. An aptamer structure switch assay coupled with horseradish peroxidase (HRP) labeling on microplates for sensitive detection of small molecule was established (Li et al., 2019). The DNA strand mediated CL platform gave us a hint that it is likely to be employed to develop a CRISPR/Cas12a-based CL biosensor on account of the trans-cleavage on ssDNA, which can indirectly or directly shear single-strand DNA coupled with native enzymes.

There is no denying that the CL signal still encounters the challenge of low detection sensitivity due to limited quantum fields. To address this constraint, signal amplification techniques have raised huge concerns such as polymerase chain reaction, strand displacement amplification, rolling circle amplification, and hybridization chain reaction (HCR) (Li et al., 2020; Yang et al., 2017; Zhang et al., 2020; Zhou et al., 2008). HCR as a potential DNA amplification technique can offer marvelous CL signal through assembling into long nicked double-stranded DNA (dsDNA) structures in various sensing systems for ultra-sensitivity detection of nucleic acids (Zhang et al., 2020). To the best of our knowledge, CL enhancement biosensor with HCR amplifying strategy has not yet been attempted in CRISPR/Cas12a system.

Inspired by the enlarged CL ability of HCR and the trans-cleavage activity of CRISPR/Cas12a, we proposed a CRISPR/Cas12a-based CL imaging sensor for ultrasensitive detection of nucleic acids by means of HCR strategy for the first time (CLE-CRISPR). The working principle of CLE-CRISPR platform was illustrated in Scheme 1. In the absence of target, the intact initiator DNA (intDNA) triggered the separation of recognition DNA (recDNA) from the assembly of MB@crDNA (formed by recognition DNA and capture DNA) via toehold-mediated DNA-strand displacement reaction (TSDR), thereby the HCR could not occur and no CL signal came out. In the presence of target, the activated CRISPR/Cas12a was capable of indiscriminately cutting intDNA into vast short products, and thus the fractured intDNA could not cause TSDR event. Therefore, the terminus of crDNA triggered the HCR with the coexistence of two hairpins (H1 and H2), forming a long double-stranded DNA framework consisting of n-(H1·H2) structure. Numerous attached streptavidin-AP yielded a robust CL signal or visual image by CCD camera directly related to the DNA target concentration. This approach feasibility was validated by analysis of synthetic DNA (snDNA) target (HPV-16 as a mode) and HPV-16 plasmid, achieving detection sensitivity for 3 pM of snDNA target and single copy per reaction of plasmid with the help of isothermal amplification (RPA), respectively. More meaningfully, the CLE-CRISPR platform was further evaluated by using 17 HPV clinical samples, exhibiting a specificity and sensitivity of 88.89% and 100%, respectively. Taken together, the proposed CRISPR-CID platform will play an essential role in the field of nucleic acids detection, and shows a promising strategy towards practical use.

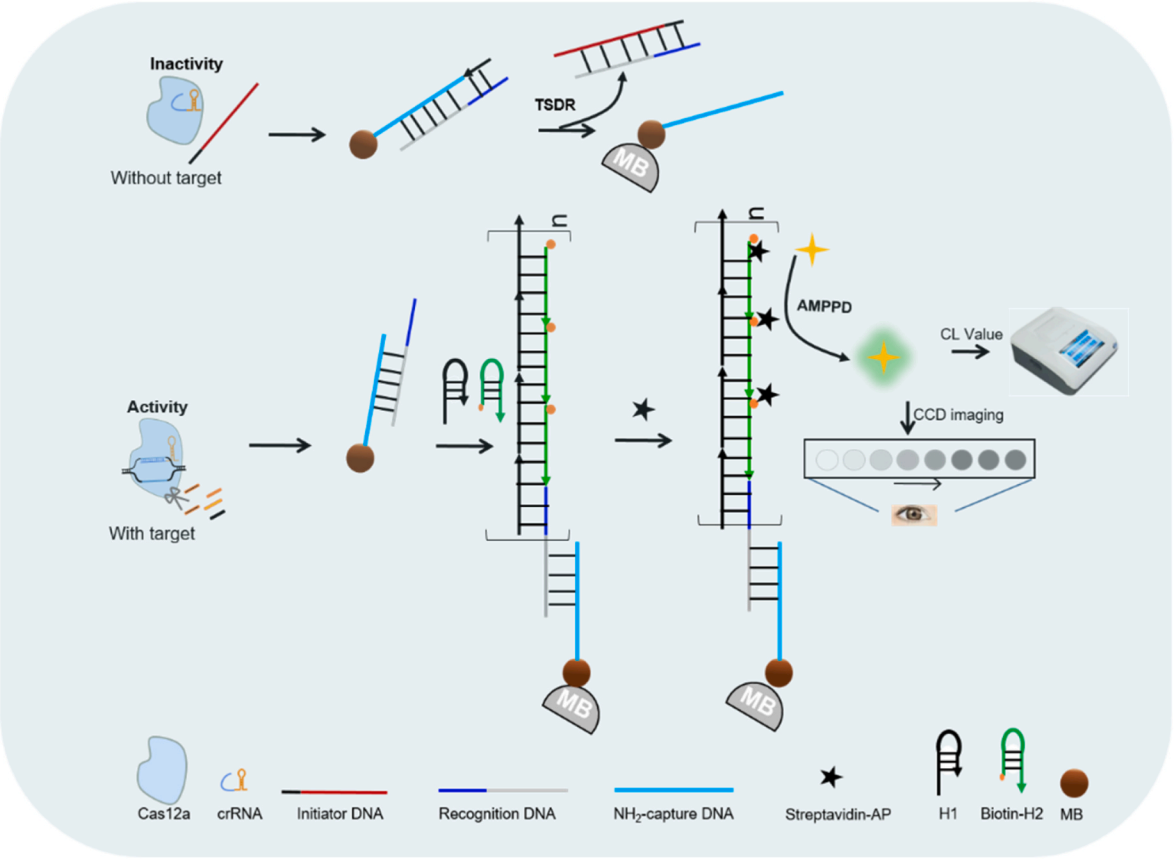

Scheme 1. The schematic diagram of the CLE-CRISPR platform for the detection of nucleic acids.

2. Experimental section

2.1. Materials and apparatus

LbCas12a was bought from Tolo Biotech (Shanghai, China). The TwistAmp Basic kit for RPA was bought from TwistDx Limited (UK). Streptavidin-AP, carboxyl coated magnetic beads (MB) (3 μm, 20 mg/mL) and magnetic rack were purchased from Beyotime Biotechnology (Shanghai, China). 3-[2-spiroadamatane]-4-methoxy-4-[3-phosphoryloxy]-phenyl-1,2-dioxetane dioxetane (AMPPD) was purchased from Ji Na Bang Sheng Lifetechnology Co., Ltd (Beijing, China). 1-ethyl-3-(3-dimethylaminopropyl) carbodiimide (EDC) and casein were obtained from Sigma-Aldrich (USA). Nucleic acids used in the study were synthesized by General Biol (Anhui) Co., Ltd (Chuzhou, China) and the sequences information of all nucleic acids were listed in Table S1. Ultrapure water (Milli-Q synthesis, Millipore Inc., Bedford, MA) was used throughout. All chemical reagents were of analytical grade.

Chemiluminescence imaging was conducted by bioanalytical imaging system (Syngene G: BOX F3 gel doc, UK). Chemiluminescence signal was recorded with a BioTek Synergy H1 (USA). Fluorescence image analysis of the beads was taken by Leica SP8 (Germany).

2.2. Preparation of MB@crDNA

NH_2-capDNA (150 nM) and recDNA (150 nM) were dissolved in MES buffer solution (pH = 6.0) and denatured at 95 °C for 5 min. Then, they were incubated at room temperature for 120 min to form crDNA. Meanwhile, MB-COOH beads (4 μL) were washed with 200 μL MES buffer solution (0.05 M, pH = 6.0) for three times and were coated with 25 μg/mL of EDC for 15 min. The beads were then washed with MES buffer solution (0.05 M, pH = 6.0) and incubated with 150 nM crDNA for 80 min. After removing the supernatant, the beads were blocked for 60 min with PBS (0.01 M, pH = 6.0) containing 0.1% tween-20 and 1% casein. The blocked beads were then washed four times and stored in PBS (0.01 M, pH = 7.0) at 4 °C for further use.

2.3. RPA assay

RPA kit was used to amplify specific target of plasmid or clinical samples. 2.4 μL forward primer (10 μM) and reverse primer (10 μM), 29.5 μL free rehydration buffer, a total volume of 13.2 μL water and template were added to the tube based on the operating instructions. Then, 2.5 μL 280 mM of MgOAc was added. The mixture was incubated at 37 °C for 30 min and was stored at 4 °C for further use.

2.4. Measurement of CLE-CRISPR

Firstly, the amplified products or snDNA target were added into the tube containing 100 nM LbCas12a-crRNA and 100 nM intDNA for 30 min at 37 °C. Then, the mixture was incubated at 95 °C for 10 min to destroy the activity of LbCas12a. The pre-prepared MB@crDNA was washed with 1 × NEBuffer 3.0 for three times and the whole above-mentioned solution was co-incubated with MB@crDNA for 60 min at room temperature. After that, 400 nM of mixture of H1 and biotin-H2 were injected. After 2 h of reaction at room temperature, the beads were washed with Tris-HCl buffer (0.02 M, 150 mM NaCl, 1 mM EDTA, 0.05% BSA, pH = 7.4) and then incubated with alkaline phosphatase (AP)-labeled streptavidin (1:5000). After incubation for 30 min, the beads were moved to 96-well plate and washed by Tris-HCl buffer (0.02 M, 150 mM NaCl, 0.05% tween 20, pH = 7.4) for five times. Finally, 100 μL of substrate for alkaline phosphatase was added into the plate and the CL intensity-time profiles were recorded. The CL signal was collected by Synergy H1 (BioTek) instrument, and simultaneously could be observed by the naked eyes via bioanalytical imaging system.

2.5. Clinical samples analysis

17 clinical samples of HPV were obtained from international peace maternity & child health hospital (Shanghai), and the diagnostic results were preferentially confirmed by human papillomavirus genotyping kit for 23 HPV Types (PCR-RDB, Reverse Dot Blot) according to operating instructions. Then, CLE-CRISPR platform was used to test 17 clinical samples.

3. Results and discussion

3.1. Characterization of TSDR and HCR efficiency and trans-cleavage of intDNA

On the basis of previous reported principle of TSDR and HCR (Wu et al., 2017; Zhou et al., 2021), the sequences of initiator DNA (intDNA), capture DNA (capDNA), recognition DNA (recDNA), hairpin DNA-1(H1) and hairpin DNA-2 (H2) were designed in this work (Table S1). In advance of initiating the TSDR process, a hybrid chain DNA (crDNA) was formed by hybridization of capDNA and recDNA through their partially complementary sequences. The TSDR between intDNA and crDNA was triggered by binding of the remaining bases of 5′-recDNA to the terminus of intDNA, resulting in the production of ciDNA formed by recDNA and intDNA, as well as the release of capDNA. The feasibility of TSDR was verified by native polyacrylamide gel electrophoresis (PAGE). As shown in Fig. 1A, Lanes 1–3 were intDNA, capDNA and recDNA bands, respectively. Lane 4 and Lane 5 individually displayed the bands of as-prepared crDNA and ciDNA. Derived from the Lane 6, the band of intDNA was nearly disappeared after co-incubation with crDNA, whereas showing an evident lower band which was in line with the position of capDNA. In addition, the upper band presented an identical position with the lane 5. Those above results obviously suggested the high performance of TSDR event triggered by intDNA, and the designed sequences were quite reasonable.

We then turned attention to HCR event induced by the single strand of recDNA. For the pure H1 and H2, different concentrations of recDNA were used to trigger the HCR and the result was illustrated in Fig. 1B. In the control groups, either alone or in mixture showed single and low bands because both H1 and H2 existed in the form of monomer, revealing that these two hairpin DNA could stably coexist in solution. After the introduction of recDNA, a series of new stripes which were higher than the positions of hairpin DNA strands could distinctly be seen on the PAGE experiment (Fig. 1B, lanes 4–8). More interestingly, the positions of these stripes changed with the concentration of recDNA while the concentration of H1and H2 were constant, which may be ascribed to the excessive recDNA competed hairpin DNA strands with each other and impeded the assembly degree. Those data demonstrated that the recDNA was capable of initiating HCR that could assemble a long double-stranded structure.

In order to further ascertain whether the MB@crDNA enabled triggering the HCR event in the presence of H1 and H2, the HCR was characterized by virtue of fluorescence microscopy analysis. The scheme of the experiment was shown in Fig. S1A, the H1-Cy5 was added into the MB@crDNA labeled with Cy3, and meanwhile the MB@crDNA was incubated with the H1-Cy5 and H2 under the same conditions. After incubation, the beads from each reaction were washed, mixed and screened by a confocal microscope for the quantization of the fluorescence intensity and the overlay of image was obtained (Fig. S1B). As displayed in Fig. 1C, the beads that underwent the HCR presented remarkable blue signal by comparison to the beads bearing only H1 in the Cy5 channel, where the Cy3 signal was used to distinguish the beads of Cy5 signal between one cycle hybridization (Cy3-crDNA and Cy5-H1) and HCR, indicating that the successful HCR event between MB@crDNA and hairpin strands. More to the point, we figured out the fluorescence intensity of HCR group was nearly 7-fold than the beads that were treated with only H1, demonstrating a high efficiency of HCR event

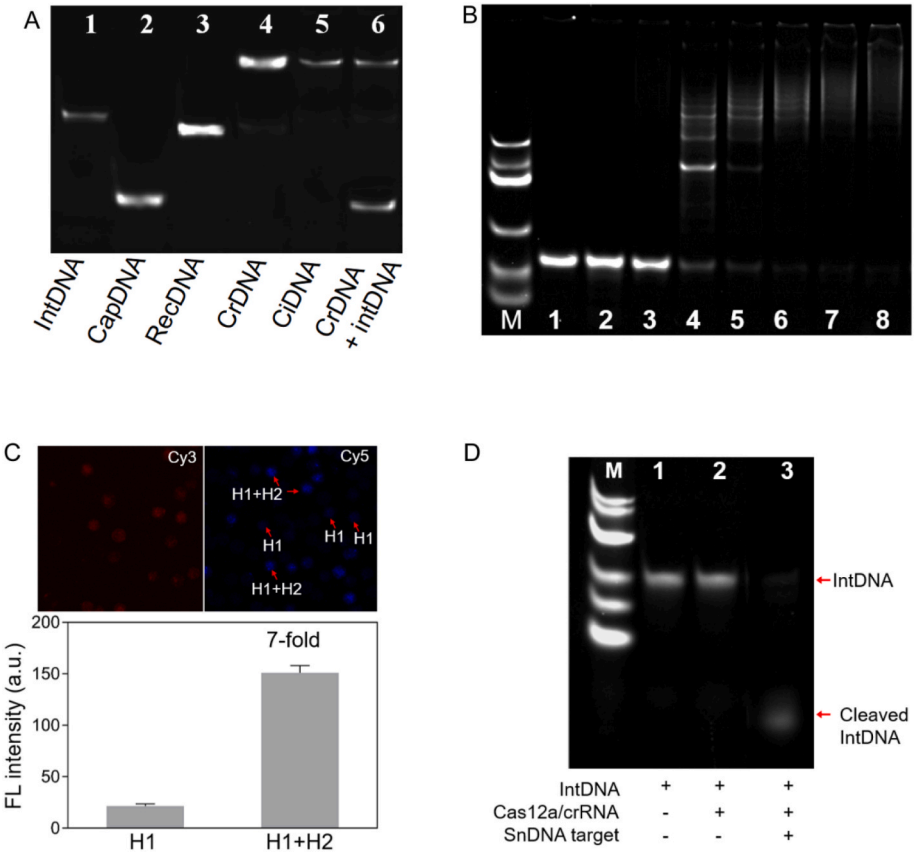

Fig. 1. (A) Native PAGE analysis of TSDR. Lane 1: intDNA, Lane 2: capDNA, Lane 3: recDNA, Lane 4: crDNA, Lane 5: ciDNA, Lane 6: crDNA + intDNA. (B) Native PAGE analysis of HCR. Lane 1: H1, Lane 2: H2, Lane 3: H1+H2, Lane 4–8: H1+H2+recDNA. The concentrations of H1 and H2 were 500 nM. The concentrations of recDNA were 500 nM, 250 nM, 200 nM, 100 nM, 50 nM from lane 4 to 8, respectively. (C) Fluorescent microscopy assay analysis of HCR (H1+H2) group versus H1 group and the FL intensity of HCR (H1+H2) group versus H1 group. (D) Denaturing PAGE characterization of the Cas12a trans-cleavage of intDNA.

between MB@crDNA and H1/H2.

To confirm whether the CL signal readout could be employed for quantification and visualization after the HCR, the terminus of H2 was modified with biotin and the CL intensity was measured. As shown in Fig. S2, a strong CL intensity or visual image were observed in the presence of MB@crDNA with the incubation of H1 and biotin-H2, while all the control groups showed negligible CL signal, revealing the feasibility of CL signal readout in this study.

It is noted that the ability of activated Cas12a to digest inDNA is extremely crucial. At this point, we used human papillomavirus 16 (HPV-16) as a model target, where the sequences of crRNA and corresponding snDNA target were listed in Table S1. To validate the trans-cleavage activity of Cas12a, a PAGE experiment was carried out. As depicted in Fig. 1D, the band of intDNA was cut into a mass of short products with the only coexistence of Cas12a/crRNA and snDNA target. The PAGE result suggested that the activated Cas12a showed high cleavage efficiency for the intDNA.

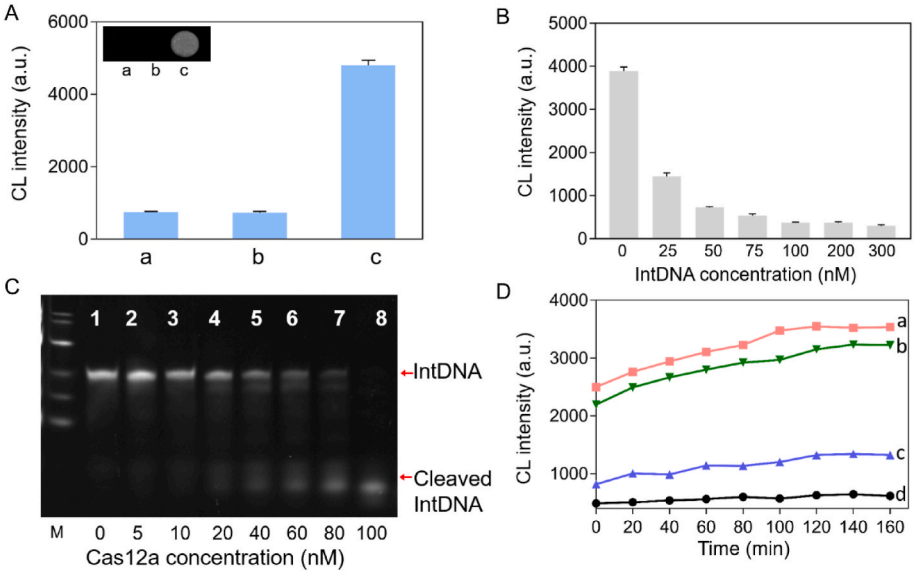

Fig. 2. (A) The feasibility of the established CLE-CRISPR platform for detection of snDNA target (Inset: visual image captured by CCD camera). a: MB@crDNA, b: MB@crDNA + intDNA + (H1/biotin-H2), c: 0.60 nM snDNA + MB@crDNA + intDNA+ (H1/biotin-H2). (B) CL intensity versus different concentrations of intDNA. (C) Denaturing PAGE analysis of the activity of Cas12a for trans-cleavage of intDNA (100 nM). (D) The CL value of the substrate catalytic as a function of time in the presence of snDNA target, a (0.50 nM), b (0.30 nM), c (0.03 nM), d (0.00 nM).

3.2. Establishment of CLE-CRISPR platform

The nucleic acids detection feasibility of CLE-CRISPR platform was confirmed through the trans-cleavage activity of Cas12a and HCR amplifying strategy. As depicted in Fig. 2A, a magnificently amplified CL signal was observed in the presence of snDNA target, while the control and blank groups showed weak CL signal. At the same time, the results could be visualized by CCD camera (Fig. 2A, inset) as well. As expected, the proposed CLE-CRISPR platform presented excellent potential for the detection of nucleic acids.

Several parameters were optimized to obtain the best performance of the CLE-CRISPR platform including the amounts of MB, the concentration of Cas12a, crDNA, intDNA, H1/H2, the reaction time of HCR and TSDR event, etc. The effect of the MB volume was initially investigated. As observed in Fig. S3A, the optimal volume of MB was 4 μL. With respect to the concentration of crDNA, it was found that the CL intensity reached a maximum at 150 nM of crDNA (Fig. S3B), which was selected for subsequent experiments. The concentration of intDNA was a key factor in the performance of the proposed method. As depicted in Fig. 2B, as the concentrations of intDNA increased from 0 to 100 nM, the CL intensity gradually decreased, and kept relatively stable from 100 nM to 300 nM, indicating that 100 nM of intDNA was sufficient to allow TSDR totally. Meanwhile, the optimal reaction time of TSDR was determined to be 60 min (Fig. S4A) under room temperature. The optimal concentration of Cas12a used for digesting 100 nM intDNA was further explored by the PAGE experiment. The results (Fig. 2C) showed that 100 nM of Cas12a could cut employed intDNA completely. The concentration of H1/bio-H2 is also a vital parameter, the optimal concentration was found to be 400 nM from an exploration of CL intensities using four different concentrations of H1/bio-H2 (Fig. S4B). In a similar fashion, both the hybridization time of HCR and the dilution concentration of streptavidin-AP were investigated. 2 h was selected to be the best HCR hybridization time (Fig. S5A) and 1:5000 dilution of streptavidin-AP (Fig. S5B) was selected for subsequent exploration. In addition, the activity of Cas12a had to be destroyed before its addition into the MB@crDNA solution in case of interfering the later experiments. The results (Fig. S5C) demonstrated that Cas12a was inactive after incubating at 95 °C for 10 min. Fig. 2D showed the impact of response time of AP substrate. When the reaction time was extended from 0 s to 120 s, the CL intensity showed an upward trend. Upon further prolonging the response time, the CL intensity kept stable, and thus the best response time was set as 120 s.

3.3. Analytical performance of sensing platform

Prior to performance analysis, a PAGE experiment demonstrated that the intDNA could be gradually digested by activated Cas12a with the increasing concentrations of snDNA (Fig. S6). Subsequently, with the aim of evaluating the analytical performance of the proposed CLE-CRISPR, the CL response in the presence of snDNA target with different concentrations were measured. Under the above optimized experimental conditions, as shown in Fig. 3A, the CL intensity increased gradually with an increase of the snDNA concentrations from 10 to 800 pM, which was also consistent with imaging changes (Fig. 3A, inset). Furthermore, the CL intensity showed good linear correlation with the snDNA concentrations ranging from 10 to 150 pM and 150–800 pM (Fig. 3A, inset). The regression equations of linear correlation between the CL values and snDNA concentrations were $CL = 11.45\ C_{snDNA} + 516$ ($R^2 = 0.9954$) and $CL = 2.87\ C_{snDNA} + 1852$ ($R^2 = 0.9943$), respectively. The limit of detection based on the 3σ/s was 3 pM, which showed excellent performance for nucleic acids detection compared with previously published works (Table S2). In order to further explore the detection sensitivity of HPV-16 plasmid, we amplified the plasmid samples ranging from 10° -10^8 copies with RPA kit (Fig. 3B, inset). Those RPA products were individually tested by CLE-CRISPR platform, and the limit of detection was single copy per reaction of HPV-16 plasmid (Fig. 3B).

3.4. Specificity and stability evaluation

To estimate the specificity of the proposed assay, the amplified HPV-18 plasmid product was used as a potential interference agent. As shown in Fig. 4A, the platform showed a remarkable CL response in the presence of amplified HPV-16 plasmid product as well as the mixtures, while the amplified HPV-18 plasmid product and the blank group showed weak CL signal. These results clearly demonstrated that this method possessed superior selectivity for discriminating the target through the crRNA-DNA manner. The stability of the method was investigated by recording the CL intensity for consecutive 10 days. As shown in Fig. 4B, The CL intensity was quite stable with a relative standard deviation (RSD) of 2.11%. In brief, the CLE-CRISPR platform proved high specificity and excellent stability during the detection of nucleic acids.

3.5. Clinical application

To illustrate the application of the CLE-CRISPR in clinical sample, the workflow of CLE-CRISPR platform for clinical sample was summarized in Fig. 5A. The designed primer sites were illustrated in Fig. S7A. The extracted nucleic acids from clinical sample were fast amplified with RPA kit, and the products were added into the solution containing Cas12a/crRNA and intDNA. The conspicuous detectable signal via HCR strategy could be read by measuring CL value or visual imaging readout. We further employed it for the detection of HPV real sample, where 17 HVP samples were tested by a commercial HPV genotyping kit for 23 types (PCR-RDB, reverse dot blot) and verifying 8 negative samples and 9 positive samples of HPV-16 (Fig. S8). As described in Fig. 5B, the results obtained from the proposed CLE-CRISPR platform were in agreement with the results for 17 samples except 1 sample. Additionally,

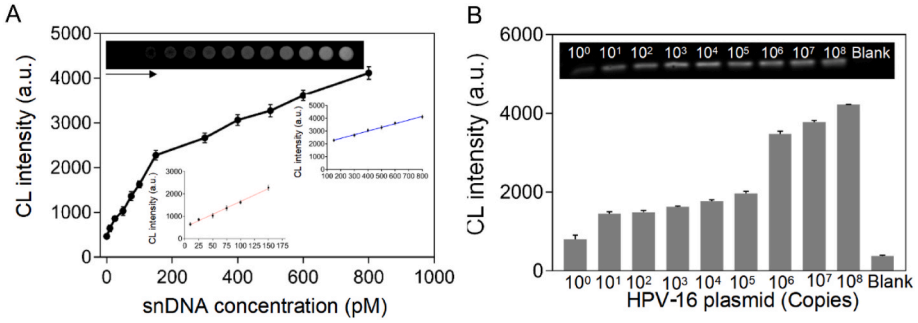

Fig. 3. (A) The CL intensity versus different concentrations of snDNA (0, 10, 25, 50, 75, 100, 150, 300, 400, 500, 600, 800 pM). (top inset: visual images changes of increasing concentrations of snDNA target; inset: correlation curves for the relationship of the CL value vs the snDNA target concentration. (B) Sensitivity of the CLE-CRISPR platform for the detection of HPV-16 plasmid with RPA kit (inset: the amplified bands from $1 \times 10^{\circ}$ to 1×10^8 copies of HPV-16 plasmid by RPA).

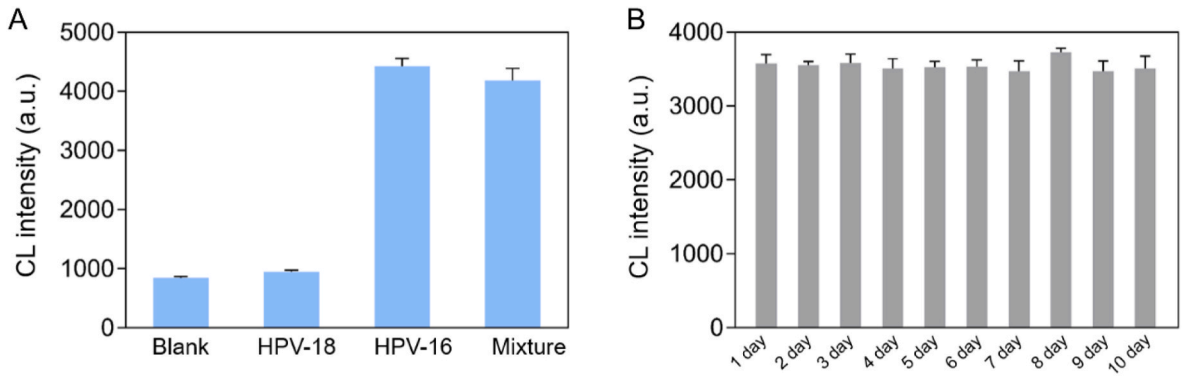

Fig. 4. (A) Evaluation of the specificity of CLE-CRISPR platform using different types of plasmids (10^4 copies). (B) The stability evaluation of the CLE-CRISPR platform.

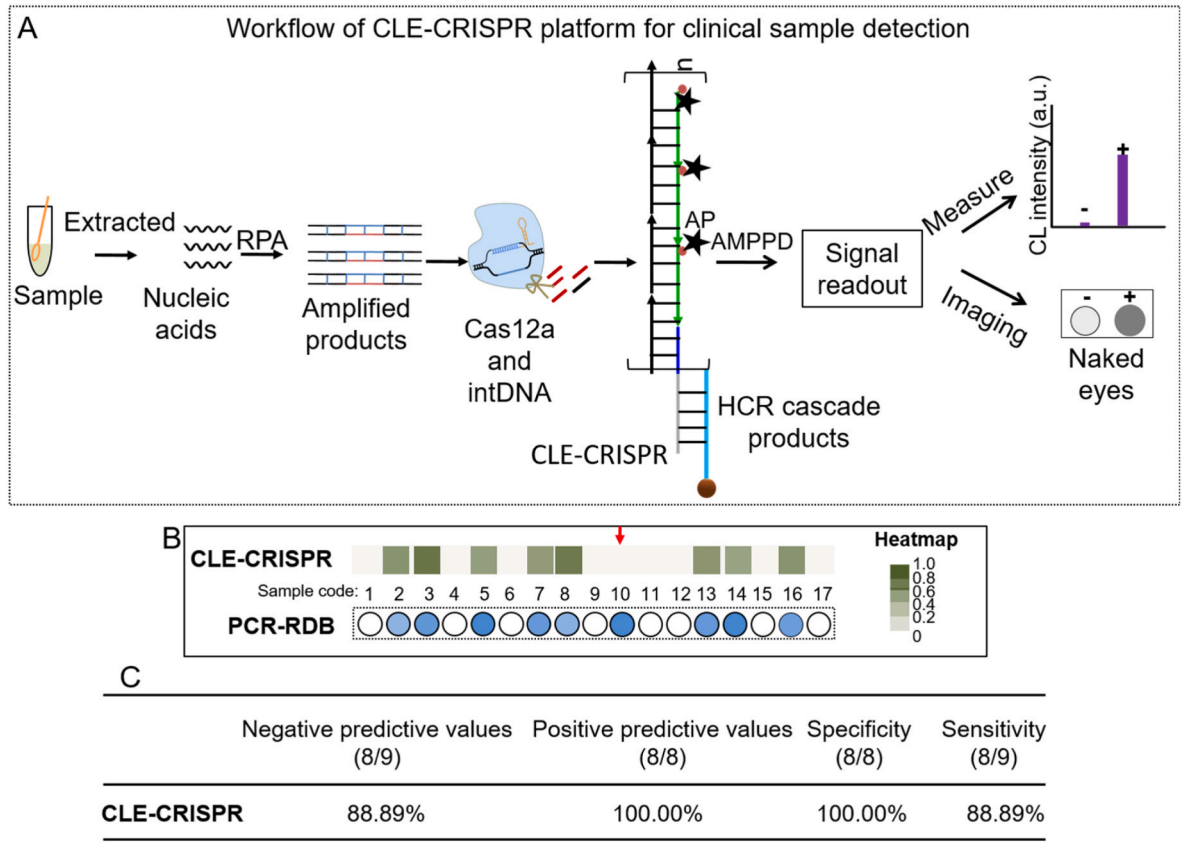

C

	Negative predictive values (8/9)	Positive predictive values (8/8)	Specificity (8/8)	Sensitivity (8/9)
CLE-CRISPR	88.89%	100.00%	100.00%	88.89%

Fig. 5. (A) Schematic diagram showing the workflow of CLE-CRISPR platform for the detection of clinical samples. (B) Heat map analysis of CLE-CRISPR platform vs PCR-RDB schematic results, the inconsistent result was shown by the red arrow. (D) Positive and negative predictive values, sensitivity, and specificity of CLE-CRISPR for clinical samples.

derived from Fig. 5C, the method exhibited excellent sensitivity and specificity of 88.89% and 100%, respectively. These results demonstrated that the CLE-CRISPR platform showed great potential in practical applications.

4. Conclusion

In summary, we first proposed a CRISPR/Cas12a triggered chemiluminescence enhancement biosensor by introducing HCR amplification strategy for the detection of nucleic acids. Owing to robust trans-cleavage of ssDNA, we utilized the CRISPR/Cas12a as an efficient biosensing system, which converts the target information into a detectable CL signal through the inherent signal amplification of HCR. Various involved factors were thoroughly investigated for constructing a high-performance of CLE-CRISPR platform. In this study, the proposed method provides high detection sensitivity of 3 pM for snDNA target and single copy per reaction for plasmid, and also exhibits excellent specificity, low-cost (Table S3). Although the CLE-CRISPR platform remains time-consuming, however, we expect improvements in the turnaround time with optimization of deactivation of Cas12a, Cas12a-crRNA engineering, and portable analysis device for signal readout.

More significantly, the proposed CLE-CRISPR platform was evaluated to test 17 clinical HPV samples by comparison with PCR-RDB gold standard. It shows superior sensitivity and specificity for clinical samples detection. Currently, the emerging SARS-CoV-2 virus has posed a great threat and burden to global public health (Dronina et al., 2021b,

2022), and thus accurate testing is essential to promote early intervention and curbs the ongoing COVID-19 pandemic. We believe that our proposed CLE-CRISPR platform, only with slight modification of crRNAs, may become an alternative method for ultra-sensitivity determination of SARS-CoV-2 or other virus induced infections. Together, we envisage that the CLE-CRISPR platform not only paves the way to construct diagnosis kit towards practical application of CRISPR-based detection technology but also gives impetus to the design of new generations of CRISPR/Cas chemiluminescence detection systems.

Ethical statement

This study has been carried out in accordance with the Code of Ethics for use of human material and information and has been approved by the ethics committee of MCHH on Human Research (Approval number: ZH2018QNA37).

CRediT authorship contribution statement

Xinxin Ke: Conceptualization, Data curation, Software, Characterization, Writing – review & editing. **Yangjing Ou:** Resources, Writing – review & editing. **Yu Lin:** Writing – review & editing. **Tao Hu:** Writing – review & editing, Conceptualization.

Declaration of competing interest

The authors declare that they have no known competing financial interests or personal relationships that could have appeared to influence the work reported in this paper.

Acknowledgement

This work was supported by the National Natural Science Foundation of China (81901536). Project of Children's Hospital Affiliated to Zhejiang University School of Medicine (Y021026).

Appendix A. Supplementary data

Supplementary data to this article can be found online at https://doi.org/10.1016/j.bios.2022.114428.

References

Ackerman, C.M., Myhrvold, C., Thakku, S.G., Freije, C.A., Metsky, H.C., Yang, D.K., Ye, S. H., Boehm, C.K., Kosoko-Thoroddsen, T.F., Kehe, J., Nguyen, T.G., Carter, A., Kulesa, A., Barnes, J.R., Dugan, V.G., Hung, D.T., Blainey, P.C., Sabeti, P.C., 2020. Massively multiplexed nucleic acid detection with Cas13. Nature 582 (7811), 277–282.

Al Yahyai, I., Al-Lawati, H.A.J., 2021. A review of recent developments based on chemiluminescence detection systems for pesticides analysis. Luminescence 36 (2), 266–277.

Chen, J.S., Ma, E., Harrington, L.B., Da Costa, M., Tian, X., Palefsky, J.M., Doudna, J.A., 2018. CRISPR-Cas12a target binding unleashes indiscriminate single-stranded DNase activity. Science 360 (6387), 436–439.

Dai, Y., Somoza, R.A., Wang, L., Welter, J.F., Li, Y., Caplan, A.I., Liu, C.C., 2019. Exploring the trans-cleavage activity of CRISPR-Cas12a (cpf1) for the development of a universal electrochemical biosensor. Angew. Chem., Int. Ed. Engl. 58 (48), 17399–17405.

Dronina, J., Bubniene, U.S., Ramanavicius, A., 2021a. The application of DNA polymerases and Cas9 as representative of DNA-modifying enzymes group in DNA sensor design. Biosens. Bioelectron. 175, 112867.

Dronina, J., Samukaite-Bubniene, U., Ramanavicius, A., 2021b. Advances and insights in the diagnosis of viral infections. J. Nanobiotechnol. 19 (1), 348.

Dronina, J., Samukaite-Bubniene, U., Ramanavicius, A., 2022. Towards application of CRISPR-Cas12a in the design of modern viral DNA detection tools. J. Nanobiotechnol. 20 (1), 41.

Feng, W., Newbigging, A.M., Tao, J., Cao, Y., Peng, H., Le, C., Wu, J., Pang, B., Li, J., Tyrrell, D.L., Zhang, H., Le, X.C., 2021. CRISPR technology incorporating amplification strategies: molecular assays for nucleic acids, proteins, and small molecules. Chem. Sci. 12 (13), 4683–4698.

Ge, H., Wang, X., Xu, J., Lin, H., Zhou, H., Hao, T., Wu, Y., Guo, Z., 2021. A CRISPR/Cas12a-Mediated dual-mode electrochemical biosensor for polymerase chain reaction-free detection of genetically modified soybean. Anal. Chem. 93 (44), 14885–14891.

Gootenberg, J.S., Abudayyeh, O.O., Lee, J.W., Essletzbichler, P., Dy, A.J., Joung, J., Verdine, V., Donghia, N., Daringer, N.M., Freije, C.A., Myhrvold, C., Bhattacharyya, R.P., Livny, J., Regev, A., Koonin, E.V., Hung, D.T., Sabeti, P.C., Collins, J.J., Zhang, F., 2017. Nucleic acid detection with CRISPR-Cas13a/C2c2. Science 356 (6336), 438–442.

Harrington, L.B., Burstein, D., Chen, J.S., Paez-Espino, D., Ma, E., Witte, I.P., Cofsky, J.C., Kyrpides, N.C., Banfield, J.F., Doudna, J.A., 2018. Programmed DNA destruction by miniature CRISPR-Cas14 enzymes. Science 362 (6416), 839–842.

Hatakeyama, K., Tanaka, T., Sawaguchi, M., Iwadate, A., Mizutani, Y., Sasaki, K., Tateishi, N., Matsunaga, T., 2009. Microfluidic device using chemiluminescence and a DNA-arrayed thin film transistor photosensor for single nucleotide polymorphism genotyping of PCR amplicons from whole blood. Lab Chip 9 (8), 1052–1058.

Horvath, P., Barrangou, R., 2010. CRISPR/Cas, the immune system of bacteria and archaea. Science 327 (5962), 167–170.

Hu, M., Yuan, C., Tian, T., Wang, X., Sun, J., Xiong, E., Zhou, X., 2020. Single-Step, salt-aging-free, and thiol-free freezing construction of AuNP-based bioprobes for advancing CRISPR-based diagnostics. J. Am. Chem. Soc. 142 (16), 7506–7513.

Jiang, Y., Hu, M., Liu, A.A., Lin, Y., Liu, L., Yu, B., Zhou, X., Pang, D.W., 2021. Detection of SARS-CoV-2 by CRISPR/Cas12a-Enhanced colorimetry. ACS Sens. 6 (3), 1086–1093.

Kricka, L.J., 2003. Clinical applications of chemiluminescence. Anal. Chim. Acta 500 (1), 279–286.

Li, L., Li, S., Wu, N., Wu, J., Wang, G., Zhao, G., Wang, J., 2019. HOLMESv2: a CRISPR-Cas12b-assisted platform for nucleic acid detection and DNA methylation quantitation. ACS Synth. Biol. 8 (10), 2228–2237.

Li, N., Fu, C., Wang, F., Sun, Y., Zhang, L., Ge, S., Zhu, P., Yu, J., 2020. Photoelectrochemical detection of let-7a based on toehold-mediated strand displacement reaction and Bi2S3 nanoflower for signal amplification. Sensor. Actuator. B Chem. 323, 128655.

Liu, S., Wang, C., Wang, Z., Xiang, K., Zhang, Y., Fan, G.C., Zhao, L., Han, H., Wang, W., 2022. Binding induced isothermal amplification reaction to activate CRISPR/Cas12a for amplified electrochemiluminescence detection of rabies viral RNA via DNA nanotweezer structure switching. Biosens. Bioelectron. 204, 114078.

Li, Y., Sun, L., Zhao, Q., 2019b. Aptamer-structure switch coupled with horseradish peroxidase labeling on a microplate for the sensitive detection of small molecules. Anal. Chem. 91 (4), 2615–2619.

Mei, S., Liu, B., Xiong, X., Hun, X., 2020. One-step fabrication of trimetallic alloy nanozyme catalyzer for luminol-H_2O_2 chemiluminescence and its application for miRNA-21 detection coupled with miRNA walking machine. J. Pharm. Biomed. Anal. 186, 113280.

Mukama, O., Wu, J., Li, Z., Liang, Q., Yi, Z., Lu, X., Liu, Y., Liu, Y., Hussain, M., Makafe, G.G., Liu, J., Xu, N., Zeng, L., 2020. An ultrasensitive and specific point-of-care CRISPR/Cas12 based lateral flow biosensor for the rapid detection of nucleic acids. Biosens. Bioelectron. 159, 112143.

Nouri, R., Tang, Z., Dong, M., Liu, T., Kshirsagar, A., Guan, W., 2021. CRISPR-based detection of SARS-CoV-2: a review from sample to result. Biosens. Bioelectron. 178, 113012.

Pickar-Oliver, A., Gersbach, C.A., 2019. The next generation of CRISPR-Cas technologies and applications. Nat. Rev. Mol. Cell Biol. 20 (8), 490–507.

Ramachandran, A., Santiago, J.G., 2021. CRISPR enzyme kinetics for molecular diagnostics. Anal. Chem. 93 (20), 7456–7464.

Smith, C.W., Nandu, N., Kachwala, M.J., Chen, Y.S., Uyar, T.B., Yigit, M.V., 2020. Probing CRISPR-Cas12a nuclease activity using double-stranded DNA-templated fluorescent substrates. Biochemistry 59 (15), 1474–1481.

Speletas, M., Kyritsi, M.A., Vontas, A., Theodoridou, A., Chrysanthidis, T., Hatzianastasiou, S., Petinaki, E., Hadjichristodoulou, C., 2020. Evaluation of two chemiluminescent and three ELISA immunoassays for the detection of SARS-CoV-2 IgG antibodies: implications for disease diagnosis and patients' management. Front. Immunol. 11, 609242.

Teng, F., Guo, L., Cui, T., Wang, X.G., Xu, K., Gao, Q., Zhou, Q., Li, W., 2019. CDetection: CRISPR-Cas12b-based DNA detection with sub-attomolar sensitivity and single-base specificity. Genome Biol. 20 (1), 132.

Urdea, M., Penny, L.A., Olmsted, S.S., Giovanni, M.Y., Kaspar, P., Shepherd, A., Wilson, P., Dahl, C.A., Buchsbaum, S., Moeller, G., Hay Burgess, D.C., 2006. Requirements for high impact diagnostics in the developing world. Nature 444 (Suppl. 1), 73–79.

Wang, Q., Liu, Y., Yan, J., Liu, Y., Gao, C., Ge, S., Yu, J., 2021. 3D DNA walker-assisted CRISPR/Cas12a trans-cleavage for ultrasensitive electrochemiluminescence detection of miRNA-141. Anal. Chem. 93 (39), 13373–13381.

Wu, Y.S., Wang, L., Jiang, W., 2017. Toehold-mediated strand displacement reaction-dependent fluorescent strategy for sensitive detection of uracil-DNA glycosylase activity. Biosens. Bioelectron. 89, 984–988.

Xu, L., Cao, Z., Ma, R., Wang, Z., Qin, Q., Liu, E., Su, B., 2019. Visualization of latent fingermarks by enhanced chemiluminescence immunoassay and pattern recognition. Anal. Chem. 91 (20), 12859–12865.

Yang, D., Tang, Y., Miao, P., 2017. Hybridization chain reaction directed DNA superstructures assembly for biosensing applications. TrAC Trends Anal. Chem. (Reference Ed.) 94, 1–13.

Yang, M., Huang, J., Fan, J., Du, J., Pu, K., Peng, X., 2020a. Chemiluminescence for bioimaging and therapeutics: recent advances and challenges. Chem. Soc. Rev. 49 (19), 6800–6815.

Yang, M., Liu, Y., Jiang, X., 2019. Barcoded point-of-care bioassays. Chem. Soc. Rev. 48 (3), 850–884.

Yang, Y., Chen, Y., Tang, H., Zong, N., Jiang, X., 2020b. Microfluidics for biomedical analysis. Small Methods 4 (4), 1900451.
Yin, L., Man, S., Ye, S., Liu, G., Ma, L., 2021. CRISPR-Cas based virus detection: recent advances and perspectives. Biosens. Bioelectron. 193, 113541.
Zhang, K., Fan, Z., Huang, Y., Ding, Y., Xie, M., 2022. A strategy combining 3D-DNA Walker and CRISPR-Cas12a trans-cleavage activity applied to MXene based electrochemiluminescent sensor for SARS-CoV-2 RdRp gene detection. Talanta 236, 122868.
Zhang, S., Li, K.B., Pan, Y., Han, D.M., 2020. Ultrasensitive detection of ochratoxin A based on biomimetic nanochannel and catalytic hairpin assembly signal amplification. Talanta 220, 121420.
Zhang, Y., Chen, M., Liu, C., Chen, J., Luo, X., Xue, Y., Liang, Q., Zhou, L., Tao, Y., Li, M., Wang, D., Zhou, J., Wang, J., 2021. Sensitive and rapid on-site detection of SARS-CoV-2 using a gold nanoparticle-based high-throughput platform coupled with CRISPR/Cas12-assisted RT-LAMP. Sensor. Actuator. B Chem. 345, 130411.
Zhou, D., Zhang, R., Fang, R., Cheng, L., Xiao, P., Lu, Z., 2008. Methylation pattern analysis using high-throughput microarray of solid-phase hyperbranched rolling circle amplification products. Electrophoresis 29 (3), 626–633.
Zhou, R., Zeng, Z., Sun, R.W., Liu, W.F., Zhu, Q.B., Zhang, X., Chen, C., 2021. Traditional and new applications of the HCR in biosensing and biomedicine. Analyst 146, 7087–7103.